Supporting Information

Cu-Erionite Zeolite Achieves High Yield in Direct Oxidation of Methane to Methanol by Isothermal Chemical Looping

Jie Zhu,[†‡§] Vitaly L. Sushkevich,[‡] Amy J. Knorpp,[†] Mark A. Newton,[†] Stefanie C. M. Mizuno,[‡] Toru Wakihara,[§] Tatsuya Okubo,[§] Zhendong Liu[*§] and Jeroen A. van Bokhoven[*†‡]

[†]Institute for Chemical and Bioengineering, ETH Zurich, Vladimir-Prelog-Weg 1, 8093 Zurich, Switzerland

[‡]Laboratory for Catalysis and Sustainable Chemistry, Paul Scherrer Institute, 5232 Villigen, Switzerland

[§]Department of Chemical System Engineering, The University of Tokyo, 7-3-1, Hongo, Bunkyo-ku, 113-8656 Tokyo, Japan

Corresponding Authors: jeroen.vanbokhoven@chem.ethz.ch (J. A. van B.)

liuzd@chemsys.t.u-tokyo.ac.jp (Z. L.)

Figure List

Figure S1 Illustration of stepwise conversion of methane to methanol including activation with oxygen, methane oxidation and extraction of methanol

Figure S2 XRD patterns and nitrogen adsorption-desorption isotherms of the Cu-ERI materials

Figure S3 SEM image of the parent ERI zeolite

Figure S4 In-situ FTIR spectra of nitrogen monoxide over Cu-ERI zeolites after activation in oxygen

Figure S5 Methanol yield over the Cu-ERI zeolites normalized by copper after reaction at 200 °C and methane partial pressure of 30 bar

Figure S6 In-situ FTIR spectra of species formed in the gas phase

Figure S7 In-situ FTIR spectra of surface species formed during reaction with methane

Figure S8 TG-DTA curves of the Cu-ERI(0.3)

Figure S9 Methanol yields of the Cu-ERI(0.3) at 300 °C in four cycles

Figure S10 XRD patterns of Cu-ERI(0.3) before oxygen activation and after reaction with methane according to the conventional procedure with a methane partial pressure of 30 bar

Figure S11 TEM images of the Cu-ERI(0.3) zeolite before and after reaction.

Supplementary Figures

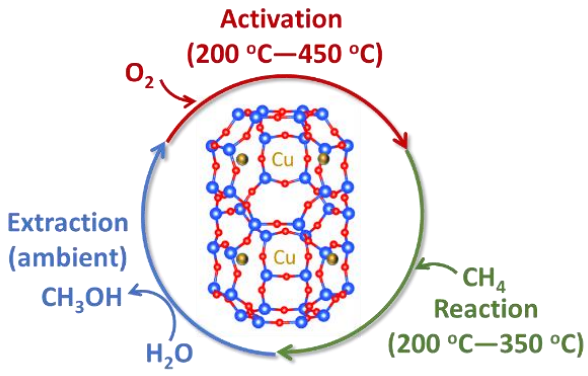

Figure S1. Illustration of stepwise conversion of methane to methanol including activation with oxygen, methane oxidation and extraction of methanol.

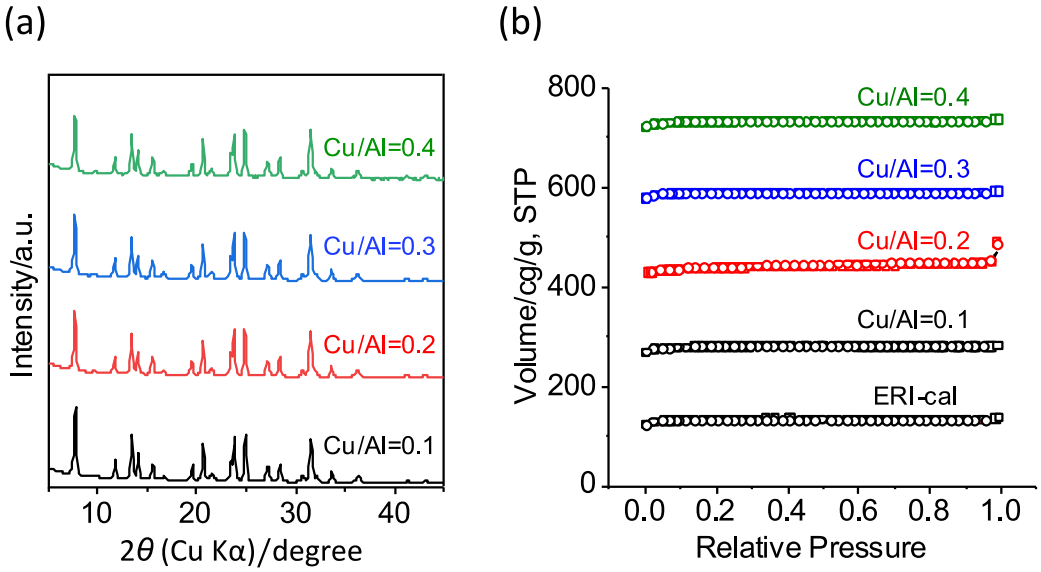

Figure S2. XRD patterns and nitrogen adsorption-desorption isotherms of the Cu-ERI materials. (a) Powder X-ray diffraction patterns of Cu-ERI zeolites with different copper loadings. (b) Nitrogen adsorption-desorption isotherms of Cu-ERI zeolites with different copper loadings.

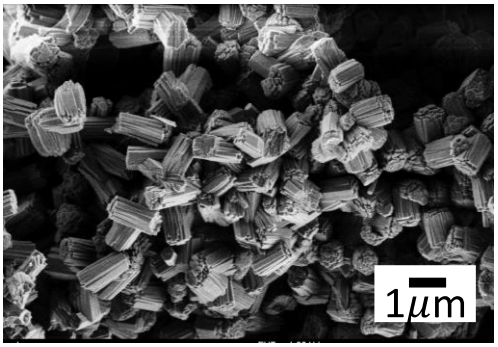

Figure S3. SEM image of the parent ERI zeolite.

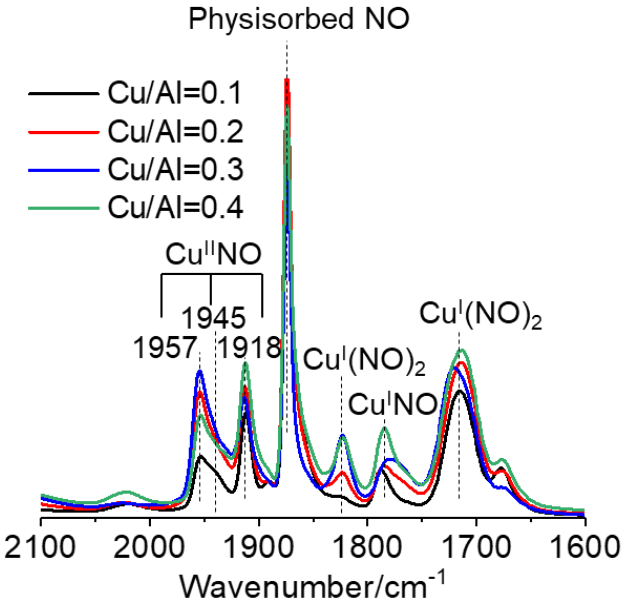

Figure S4. In-situ FTIR spectra of nitrogen monoxide over Cu-ERI zeolites after activation in 300 torr of oxygen at 673 K for 1 h.

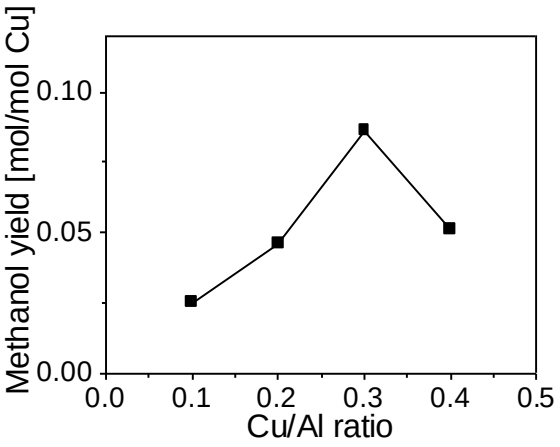

Figure S5. Methanol yield over the Cu-ERI zeolites normalized by copper after reaction at 200 °C and methane partial pressure of 30 bar.

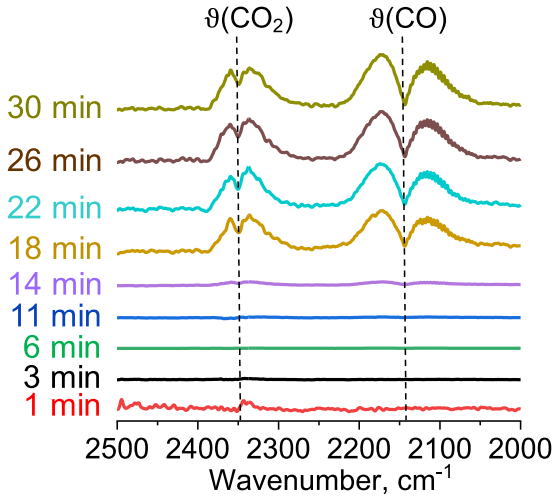

Figure S6. In-situ FTIR spectra of surface species formed after the reaction with methane at different temperatures for 30 min.

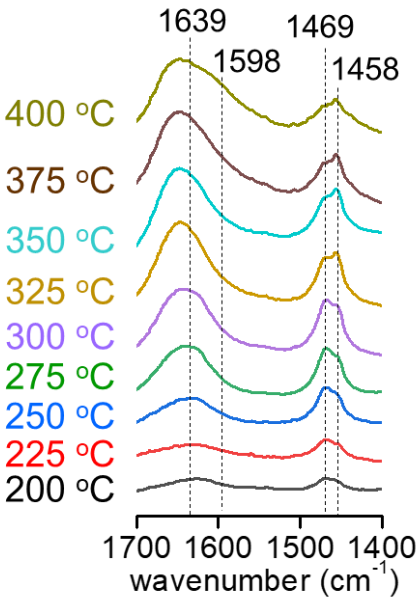

Figure S7. In-situ FTIR spectra of species formed in the gas phase through the reaction with methane in 30 min at 300 °C. The amount of carbon monoxide and carbon dioxide formed as gas phase are calculated as 9.4 μmol/g-zeolite and 2.5 μmol/g-zeolite, respectively. A methanol yield of 80 μmol/g-zeolite was achieved, thus the selectivity for Cu-ERI(0.3) was caculated as $\frac{80\ \mu mol/g-zeolite}{(80+9.4+2.5)\ \mu mol/g-zeolite} = 87\%$.

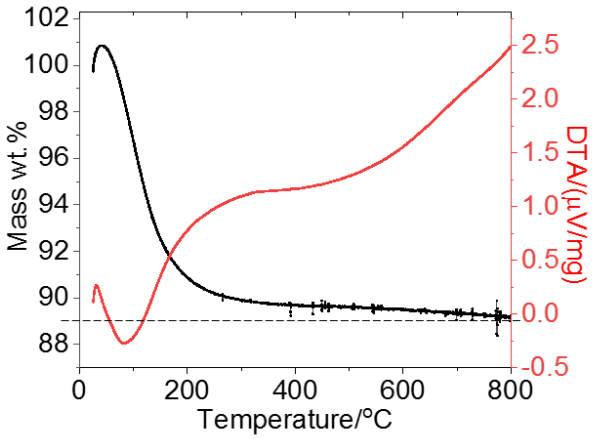

Figure S8. TG-DTA curves of the Cu-ERI(0.3).

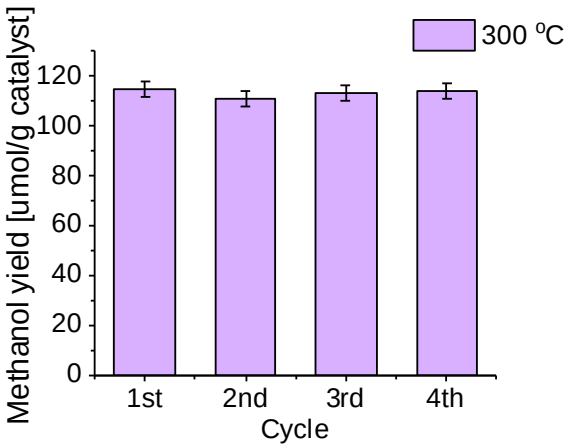

Figure S9. Methanol yields of the Cu-ERI(0.3) at 300 °C in four cycles. (Note that only one methanol extraction was performed to calculate the methanol yield.)

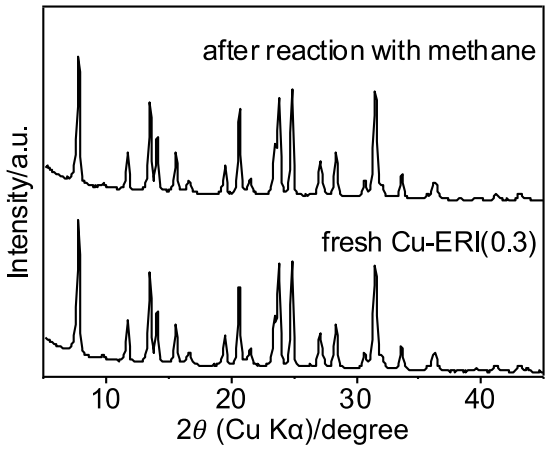

Figure S10. XRD patterns of Cu-ERI(0.3) before activation and after reaction according to the conventional procedure with methane partial pressure of 30 bar.

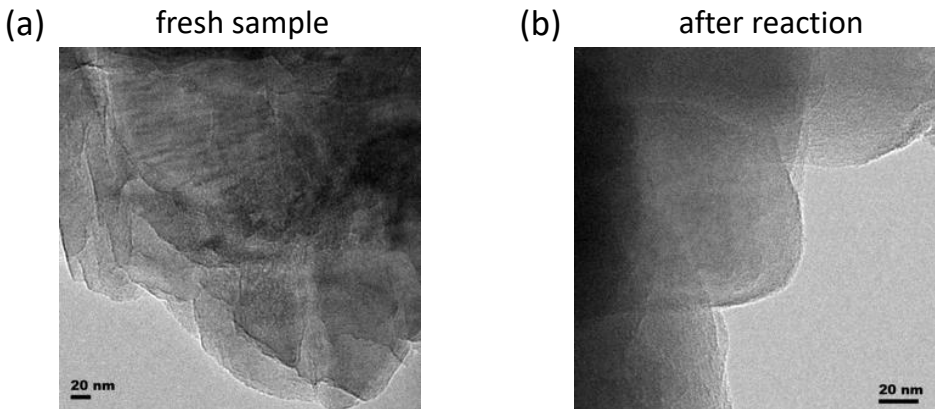

Figure S11. TEM images of the Cu-ERI(0.3) zeolite before and after reaction. (a) Before activation in oxygen. (b) After the reaction according to the conventional procedure at a methane partial pressure of 30 bar.